Title

Dephosphorylation of Tyrosine 393 in Argonaute 2 by Protein Tyrosine Phosphatase 1B Regulates Gene Silencing in Oncogenic RAS-Induced Senescence

Journal

Molecular Cell, 55(5)

ISSN

1097-2765

Authors

Yang, Ming
Haase, Astrid D
Huang, Fang-Ke
et al.

Publication Date

2014-09-01

DOI

10.1016/j.molcel.2014.07.018

Peer reviewed

Molecular Cell
Short Article

Dephosphorylation of Tyrosine 393 in Argonaute 2 by Protein Tyrosine Phosphatase 1B Regulates Gene Silencing in Oncogenic RAS-Induced Senescence

Ming Yang,[1,2] Astrid D. Haase,[1,3] Fang-Ke Huang,[4] Gérald Coulis,[5,6] Keith D. Rivera,[1] Bryan C. Dickinson,[3,7] Christopher J. Chang,[3,7] Darryl J. Pappin,[1] Thomas A. Neubert,[4] Gregory J. Hannon,[1,3] Benoit Boivin,[1,5,6,8,*] and Nicholas K. Tonks[1,8,*]

[1]Cold Spring Harbor Laboratory, Cold Spring Harbor, NY 11724, USA
[2]Department of Biochemistry and Cell Biology, Stony Brook University, Stony Brook, NY 11790, USA
[3]Howard Hughes Medical Institute
[4]Department of Biochemistry and Molecular Pharmacology, Kimmel Center for Biology and Medicine at the Skirball Institute, New York University Langone School of Medicine, New York, NY 10016, USA
[5]Department of Biochemistry and Department of Medicine, Université de Montréal, Montréal, H3C 3J7 QC, Canada
[6]Montreal Heart Institute, Montréal, H1T 1C8 QC, Canada
[7]Departments of Chemistry and Molecular and Cell Biology, University of California, Berkeley, Berkeley, CA 94720, USA
[8]Co-senior author
*Correspondence: benoit.boivin@icm-mhi.org (B.B.), tonks@cshl.edu (N.K.T.)
http://dx.doi.org/10.1016/j.molcel.2014.07.018

SUMMARY

Oncogenic *RAS* (H-RAS^{V12}) induces premature senescence in primary cells by triggering production of reactive oxygen species (ROS), but the molecular role of ROS in senescence remains elusive. We investigated whether inhibition of protein tyrosine phosphatases by ROS contributed to H-RAS^{V12}-induced senescence. We identified protein tyrosine phosphatase 1B (PTP1B) as a major target of H-RAS^{V12}-induced ROS. Inactivation of PTP1B was necessary and sufficient to induce premature senescence in H-RAS^{V12}-expressing IMR90 fibroblasts. We identified phospho-Tyr 393 of argonaute 2 (AGO2) as a direct substrate of PTP1B. Phosphorylation of AGO2 at Tyr 393 inhibited loading with microRNAs (miRNAs) and thus miRNA-mediated gene silencing, which counteracted the function of H-RAS^{V12}-induced oncogenic miRNAs. Overall, our data illustrate that premature senescence in H-RAS^{V12}-transformed primary cells is a consequence of oxidative inactivation of PTP1B and inhibition of miRNA-mediated gene silencing.

INTRODUCTION

Reactive oxygen species (ROS) play complex roles in signal transduction, including promoting the indirect regulation of tyrosine phosphorylation-dependent cascades (Finkel, 2011). In response to the regulated and localized generation of ROS as second messenger molecules, transient oxidation of the catalytic cysteine of a subset of protein tyrosine phosphatases (PTPs) facilitates signaling (Tonks, 2013). Reversible oxidation causes the remodeling of the PTP active site, abrogates the nucleophilicity of the conserved catalytic cysteine residue toward phosphorylated substrates, and tips the delicate equilibrium between protein tyrosine kinase and phosphatase activity in favor of tyrosine phosphorylation. Since the conserved cysteine residue is present in all 105 members of the human PTP family, the inactivation of individual PTPs has been reported in a wide array of cellular processes including cell growth and cell motility and in the etiology of several diseases including diabetes and cancer (Julien et al., 2011; Tonks, 2013).

Cancer has been described as a multistep disease in which normal cells progressively acquire traits that enable them to become tumorigenic (Hanahan and Weinberg, 2000). It is increasingly clear that, based on its level of expression, activation of an oncogene induces either proliferation (at low levels) or premature senescence (at elevated levels) in primary cells in culture and in vivo (Collado and Serrano, 2010; Ferbeyre, 2007; Serrano et al., 1997). Hence, one of the traits required for tumorigenesis is to allow cells to bypass the G_1 cell-cycle arrest that characterizes oncogenic senescence (Collado and Serrano, 2010).

Approximately 30% of human cancers harbor somatic gain-of-function mutations in *RAS* genes (Schubbert et al., 2007). Interestingly, primary cells expressing high levels of oncogenic RAS undergo a rapid, telomere-independent, ROS-, p53-, and p16^{INK4a}-dependent senescence program (Lee et al., 1999; Serrano et al., 1997). Although previously seen as a reaction by-product causing oxidative stress, ROS, and in particular hydrogen peroxide (H_2O_2), are now considered to be bona fide small-molecule second messengers involved in the regulation of cellular homeostasis (Rhee, 2006). RAS signaling induces the controlled single-electron reduction of molecular oxygen to superoxide (Irani et al., 1997) through the acute activation of NADPH oxidases (Brown and Griendling, 2009). Superoxide is then rapidly converted to the more stable and membrane permeant oxygen derivative H_2O_2 by spontaneous or enzymatic

dismutation (Brown and Griendling, 2009). ROS can directly damage DNA and trigger the DNA damage responses, or promote the stabilization of both p53 mRNA and protein (DeNicola and Tuveson, 2009). Hence, it is thought that ROS production is an essential element of cell-cycle arrest induced by oncogenic RAS (DeNicola and Tuveson, 2009). Although the molecular mechanism of ROS-induced senescence is unknown, it has the potential to involve the reversible redox inactivation of members of the PTP family. In testing this hypothesis, we demonstrated that PTP1B was reversibly oxidized and inactivated in human diploid fibroblasts expressing high levels of oncogenic H-RAS^{V12}. We observed that the inactivation of PTP1B led to hyperphosphorylation of argonaute 2 (AGO2) on Tyr 393. Recently, it was shown that phosphorylation of AGO2 on Tyr 393 decreases its interaction with DICER and inhibits the maturation of miRNA (Shen et al., 2013). Here we have shown that this modification prevented miRNA loading on AGO2, compromised the regulation of p21 mRNA, and induced senescence. These findings shed light on the role of PTP1B in senescence and on how ROS signaling is tightly linked to miRNA-mediated posttranscriptional regulation.

RESULTS

Premature Senescence Induced by Oncogenic RAS via Reversible Oxidation of PTP1B

Generation of ROS is thought to be an integral part of the signaling pathways leading to oncogene-induced cell-cycle arrest (DeNicola and Tuveson, 2009). In order to identify PTPs that are inactivated by ROS and might contribute to oncogene-induced senescence, we performed a modified cysteinyl-labeling assay (Boivin et al., 2008, 2010) on low-passage human diploid fibroblasts (IMR90) in which an activated *RAS* allele (*H-RAS*^{V12}) was introduced by a retroviral vector (Serrano et al., 1997). Cells from this well-characterized oncogene-induced senescence model developed a flat and enlarged morphology and demonstrated senescence-associated β-galactosidase (SA β-gal) activity at day 6 post puromycin selection, as described previously (Serrano et al., 1997) (Figure 1A). In addition, using peroxyfluor-6 acetoxymethyl ester (PF6-AM), an H_2O_2-specific fluorescence indicator (Dickinson et al., 2011), and Amplex red, which is converted to a fluorescent derivative in presence of H_2O_2, we observed an H-RAS^{V12}-induced increase in H_2O_2 that was consistent with the SA β-gal activity (Figures 1B and 1C). Since PTPs are inactivated by H_2O_2, we investigated whether specific members of this family were reversibly oxidized in senescent fibroblasts. The cysteinyl-labeling assay converts the reversible oxidation of PTPs to a modification by biotin that can be visualized by immunoblotting after a biotin-streptavidin high-affinity purification step (Boivin et al., 2008, 2010). As shown in Figure 1D, minimal biotin labeling was observed in normal fibroblasts; however, biotinylation was detected in lysates of H-RAS^{V12}-expressing fibroblasts, with an ~50 kDa protein displaying pronounced reversible oxidation when compared to normal fibroblasts. Immunoblotting the streptavidin-purified samples from the cysteinyl-labeling assay for PTPs of ~50 kDa revealed that PTP1B was targeted by H_2O_2 in RAS-induced senescent (Figure 1E) or replicative senescent (Figure S1A) human diploid fibroblasts. This was confirmed using scFv antibodies that selectively recognize the oxidized, inactive form of PTP1B, which indicated that the extent of reversible oxidation of endogenous PTP1B was ~50% in H-Ras^{V12}-expressing cells (Figure S1B).

A time-dependent increase in PTP1B oxidation was detected in H-RAS^{V12}-expressing cells (Figure 1F), and pretreatment with the ROS scavenger N-acetylcysteine (NAC) markedly decreased oxidation of PTP1B. Previous studies demonstrated that the levels of the cyclin-dependent kinase inhibitor p21, a target of p53, were increased in primary fibroblasts expressing H-RAS^{V12} (Serrano et al., 1997). We observed that p21 expression was also compromised by NAC treatment (Figure 1F). This indicates that both PTP1B activity and p21 expression were regulated by ROS downstream of H-RAS^{V12}.

To test if PTP1B inactivation was essential for the onset of oncogene-induced senescence, we coinfected IMR90 cells with *H-RAS*^{V12} and a virus encoding either active or catalytically inactive PTP1B (PTP1B CS). More than 70% of H-RAS^{V12}-expressing fibroblasts exhibited SA β-gal activity (Figure 1G). In contrast, cells overexpressing the active phosphatase, which compensated for the pool of ROS-inactivated enzyme (Figure S1C), displayed a 4-fold reduction in senescence, whereas the catalytically impaired PTP1B mutant did not affect the appearance of RAS-induced SA β-gal activity. Furthermore, we treated RAS-expressing IMR90 cells with MSI-1436 and CPT-157633, inhibitors of PTP1B with distinct structures and mechanisms of inhibition (Krishnan et al., 2014; Mark et al., 2006). At day 2, when RAS signaling was active, but ROS levels and oxidation of PTP1B were still low, inhibition of PTP1B caused a 2-fold increase in β-gal-positive cells (Figures 1H, S1D, and S1E). Moreover, specifically inhibiting PTP1B with MSI-1436 in NAC-treated cells at day 6, which mimics low-ROS conditions, was sufficient to offset the NAC inhibition of H-RAS^{V12}-induced senescence previously reported by others (Lee et al., 1999) (Figure 1I). This demonstrates a critical role of the reversible oxidation of PTP1B in triggering RAS-induced senescence.

AGO2 Was a Major Substrate of PTP1B in H-RAS^{V12}-Induced Senescence

We reasoned that since the inhibition of PTP1B was required for H-RAS^{V12}-induced senescence, critical substrates should be hyperphosphorylated in these conditions. To identify these targets, we used a PTP1B substrate-trapping mutant to identify its physiological substrates in IMR90 cells expressing H-RAS^{V12} (Tonks, 2013). We used liquid chromatography-tandem mass spectrometry (LC-MS/MS) to identify those proteins that associated with substrate-trapping mutant PTP1B (DA) or catalytically competent PTP1B (WT) that was immunoprecipitated from cellular extracts of control or H-RAS^{V12}-expressing IMR90 cells. AGO2 was the most abundant protein found in a complex with the substrate-trapping mutant in H-RAS^{V12}-expressing fibroblasts compared to the WT enzyme (Table S1). A similar enrichment of AGO2 bound to PTP1B DA (> 8 fold) was also observed when comparing lysates of cells in the presence and absence of H-RAS^{V12} (Table S2).

Argonaute proteins and their associated miRNAs silence gene expression at posttranscriptional levels in animals, and were

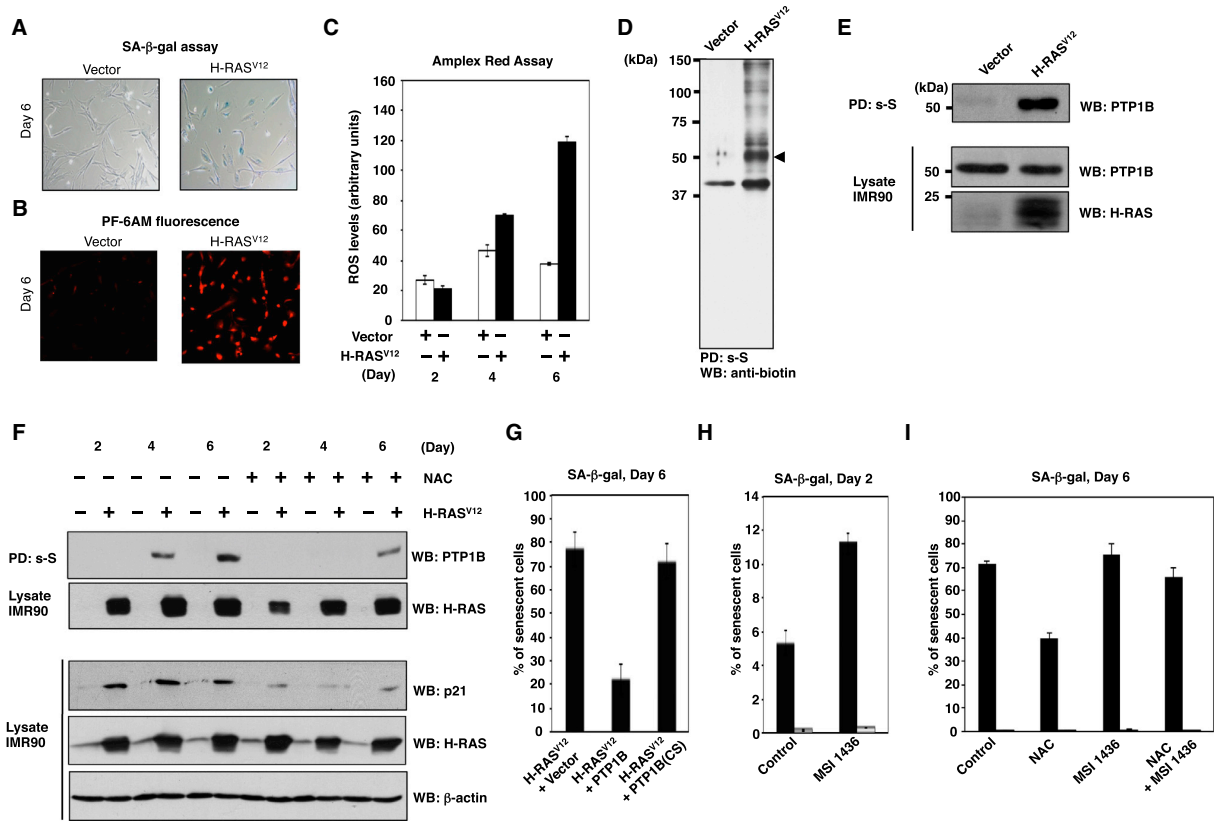

Figure 1. PTP1B Oxidation Was Required for H-RAS^{V12}-Induced Senescence

(A) Representative photographs of IMR90 fibroblasts stained for SA β-gal activity.

(B) H-RAS^{V12}-induced H_2O_2 production was assessed by molecular imaging using PF6-AM.

(C) Levels of H_2O_2 released in the culture medium of *H-RAS*^{V12}-transformed cells were quantitated by Amplex red.

(D) Control or H-RAS^{V12}-induced senescent cells were subjected to the cysteinyl-labeling assay, using biotinylated IAP at pH 5.5. Biotinylated proteins were purified on streptavidin-Sepharose beads, resolved by SDS-PAGE, and visualized using anti-biotin HRP.

(E) Proteins enriched in the cysteinyl-labeling assay were resolved by SDS-PAGE and immunoblotted using an anti-PTP1B antibody (FG6) (upper panel). Total PTP1B and H-RAS^{V12} expression levels were measured by immunoblotting 5% of the lysate.

(F) Control or H-RAS^{V12}-induced senescent cells were cultured with or without 1 mM N-acetylcysteine (NAC) for 2, 4, or 6 days, then subjected to the cysteinyl-labeling assay. Reversibly oxidized PTP1B was visualized using FG6. Total H-RAS^{V12} and p21 expression levels were measured by immunoblotting 5% of the lysate.

(G) Cells infected with *H-RAS*^{V12} and *PTP1B* (WT) or a catalytically impaired PTP1B mutant (*PTP1B* [CS]) were stained for β-gal activity following a 2-day puromycin selection (H-RAS^{V12}) and 6-day hygromycin selection (PTP1B).

(H) Control (white bars) or H-RAS^{V12}-expressing (black bars) cells were cultured in the presence or absence of the PTP1B inhibitor, MSI-1436 (20 μM). Cells were stained for β-gal activity 2 days postpuromycin selection.

(I) Control (white bars) or H-RAS^{V12}-expressing (black bars) cells were cultured in the absence or in the presence of 1 mM NAC, 20 μM MSI-1436, or both, for a 6 day period postselection. In samples stained for β-gal activity, cells were counted and expressed as the percentage of senescent cells in the total population. Error bars represent SEM of three independent experiments.

recently implicated in senescence (Gorospe and Abdelmohsen, 2011). To investigate whether PTP1B was involved in the regulation of miRNA-mediated gene silencing, we tested the interaction of PTP1B (WT), or the substrate-trapping mutant PTP1B (DA), with components of the RNA-induced silencing complex (RISC). Interestingly, AGO2, but not AGO1, 3, and 4 or other components of the RISC (DICER and TRBP), was specifically enriched with PTP1B (DA) in HEK293 cells (Figure S2B). We estimated that ~34% of the total AGO2 interacted with the PTP1B-trapping mutant in H-RAS^{V12}-expressing cells (Figure 2A). As expected from this result, we observed that AGO2 was tyrosine phosphorylated in H-RAS^{V12}-expressing cells, as well as in replicative senescent cells (Figure S1A), and expression of WT PTP1B decreased tyrosine phosphorylation of AGO2 (Figure 2B). By testing known (Y393, Y529) (Rüdel et al., 2011) and predicted (Y55, Y57, Y741) phosphorylation sites on AGO2 (Figure 2C), we identified tyrosines 393 and 529 as the main sites in H-RAS^{V12}-expressing HEK293 cells (Figures 2D

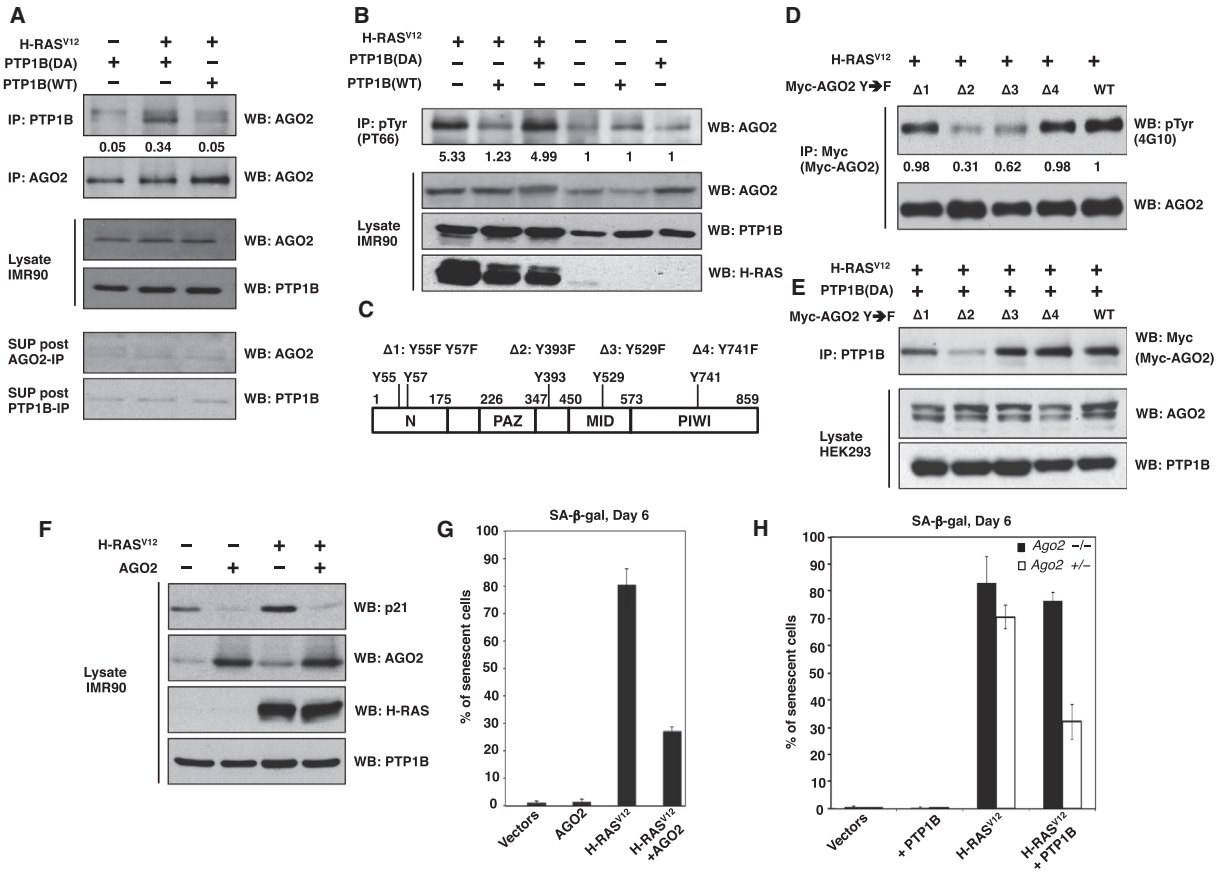

Figure 2. PTP1B Dephosphorylated AGO2 on Tyr 393

(A) Lysates were prepared from cells expressing PTP1B (DA), H-RAS^{V12} and PTP1B (DA), or H-RAS^{V12} and PTP1B (wild-type [WT]). PTP1B was immunoprecipitated from half of each lysate, whereas total AGO2 was immunoprecipitated from the second half. Immunoprecipitates were blotted with an anti-AGO2 antibody, to estimate the stoichiometry of association between AGO2 and PTP1B. A total of 5% of the supernatant recovered after the immunoprecipitation (post-IP) and same amount of lysate was resolved by SDS-PAGE and blotted for AGO2 and PTP1B to illustrate the efficiency of immunoprecipitation.

(B) pTyr proteins were immunoprecipitated from lysates of cells expressing the indicated combination of H-RAS^{V12} and PTP1B proteins using the PT-66 antibody. The precipitates were then resolved and blotted for AGO2. Lysates were blotted for the total expression of AGO2, PTP1B (WT or DA), and H-RAS. Images were analyzed using ImageJ.

(C) Schematic representation of AGO2 domains identifying the five tyrosine residues that were mutated to phenylalanine.

(D) Myc-tagged AGO2, either WT or phosphorylation site mutants ([1]Y55F,Y57F; [2]Y393F; [3]Y529F; [4]Y741F), was expressed in HEK293 cells together with H-RAS^{V12}, then immunoprecipitated using an anti-Myc antibody and blotted for the presence of phosphorylated tyrosine using 4G10. The membrane was stripped and reblotted for total AGO2.

(E) Immunoblot of Myc-tagged AGO2, either WT or phosphorylation site mutants ([1]Y55F,Y57F; [2]Y393F; [3]Y529F; [4]Y741F), to demonstrate interaction with the PTP1B (DA) substrate-trapping mutant in H-RAS^{V12}-expressing HEK cells. Lysates were resolved by SDS-PAGE, and transferred and blotted for AGO2 and PTP1B to illustrate equal expression of the mutant proteins.

(F) IMR90 cells infected with the control vector, *AGO2*, *H-RAS*^{V12}, or both were lysed and blotted for p21, AGO2, H-RAS, and PTP1B.

(G) β-gal activity was measured in IMR90 cells infected with the control vectors, *AGO2*, *H-RAS*^{V12}, or both. Senescent cells were counted as β-gal-positive cells relative to total cells.

(H) Nonimmortalized *Ago2* knockout (*Ago2* −/−, black bars) and heterozygous (*Ago2* +/−, white bars) MEFs coinfected with control vectors, *PTP1B*, *H-RAS*^{V12}, or with *H-RAS*^{V12} and *PTP1B* were cultured for 6 days postselection and stained for β-gal activity. Senescent cells were counted as β-gal-positive cells relative to the total cells. Images were quantitated using ImageJ. Error bars represent SEM (n = 3).

and S2C). Furthermore, through generation of a phosphospecific antibody, we demonstrated H-RAS^{V12}-induced phosphorylation of Tyr 393 (Figures S2D and S2E). Accordingly, the AGO2-PTP1B (DA) complex was dependent upon the phosphorylation of AGO2 on Tyr 393 in substrate-trapping experiments (Figure 2E). Taken together, our results indicate that Tyr 393 of AGO2 is hyperphosphorylated in response to PTP1B inactivation and may contribute to H-RAS^{V12}-induced development of senescence. To test this hypothesis, first we compensated for the potential inactivating tyrosine phosphorylation of AGO2 by

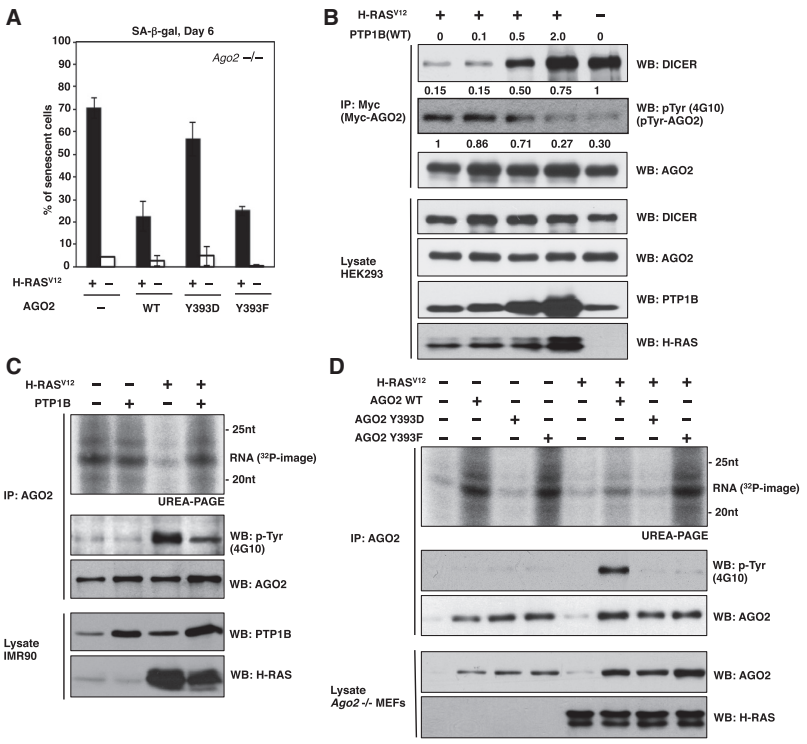

Figure 3. PTP1B Prevented H-RAS^{V12}-Induced Senescence by Dephosphorylating AGO2

(A) Nonimmortalized *Ago2* −/− MEFs infected with *H-RAS*^{V12} (black bars) or the control vector (white bars) were coinfected with a control vector, *AGO2* WT, or mutants (Y393D, Y393F), cultured for 6 days postselection, and stained for β-gal activity. Senescent cells were counted as β-gal-positive cells relative to the total cells.

(B) Myc-tagged AGO2 was immunoprecipitated from cell lysates of untransfected HEK293 or from HEK293 cells cotransfected with *H-RAS*^{V12} and 0, 0.1, 0.5, or 2.0 μg of *PTP1B* (WT) expression plasmid, resolved by electrophoresis, and blotted for DICER, AGO2 tyrosine phosphorylation (4G10), and total AGO2. Lysates were also blotted for PTP1B and H-RAS.

(C) AGO2 was immunoprecipitated from lysates of control IMR90 cells, cells expressing H-RAS^{V12}, cells expressing PTP1B, or cells expressing both H-RAS^{V12} and PTP1B, and associated RNAs were extracted, 5′-end labeled with [γ-^{32}P]-ATP, and resolved by electrophoresis. Labeled miRNAs were visualized by autoradiography (top panel).

(D) AGO2 was immunoprecipitated from lysates of immortalized *Ago2* −/− MEFs infected with *AGO2* WT or mutants (Y393D, Y393F) with or without *H-RAS*^{V12}, and associated RNAs were extracted, 5′-end labeled with [γ-^{32}P]-ATP, resolved by electrophoresis, and labeled miRNAs were visualized by autoradiography (top panel). In (C) and (D), AGO2 was immunoprecipitated from 10% of the lysates to illustrate AGO2 tyrosine phosphorylation and total levels. A total of 5% of the input lysates were blotted for AGO2 and H-RAS. Images were quantitated using ImageJ. Error bars represent SEM (n = 3).

overexpressing AGO2 in H-RAS^{V12}-expressing primary fibroblasts; we observed that overexpression of AGO2 inhibited p21 expression (Figure 2F) and senescence (Figure 2G). Second, we examined whether PTP1B could rescue H-RAS^{V12}-induced senescence in *Ago2*-null (*Ago2* −/−) mouse embryonic fibroblasts (MEFs) and in *Ago2*-heterozygous (*Ago2* +/−) MEFs. We observed that overexpression of PTP1B only prevented H-RAS^{V12}-induced senescence when AGO2 was expressed (Figure 2H). This is consistent with an ROS-PTP1B-AGO2 pathway that was responsible for H-RAS^{V12}-induced senescence.

Phosphorylation of AGO2 on Tyr 393 Was Necessary and Sufficient for H-RAS^{V12}-Induced Senescence

To determine the importance of tyrosine phosphorylation of AGO2 in its ability to suppress senescence, we overexpressed WT or Tyr 393 mutants (AGO2 Y393D, AGO2 Y393F) in H-RAS^{V12}-expressing *Ago2*-null (*Ago2* −/−) MEFs (Figure S3) and quantitated the effects on H-RAS^{V12}-induced senescence. The AGO2 Y393D mutant possesses an additional negative charge, which would partially mimic the phosphorylated form of AGO2 that would occur when PTP1B was inactivated; as expected, overexpression of the AGO2 Y393D mutant did not prevent RAS-induced senescence (Figures 3A and S3). In contrast, overexpression of the AGO2 mutant (AGO2 Y393F), which cannot be phosphorylated, prevented the appearance of senescence to a similar extent to the WT enzyme. This suggests that an inhibitory tyrosine phosphorylation of AGO2 is an important feature of its ability to rescue the *Ago2*-deficient MEFs from RAS-induced senescence.

AGO2 Tyrosine 393 Phosphorylation Prevented miRNA Loading

Tyr 393 of AGO2 is located close to the interaction domain with DICER, and phosphorylation of this residue impairs binding of AGO2 to DICER (Meister, 2013; Shen et al., 2013). Indeed, we observed that the AGO2-DICER interaction was impaired in H-RAS^{V12}-expressing cells (Figure 3B) and that overexpression of PTP1B restored the association. Since the association of DICER and AGO2 is required for loading of AGO2 with mature miRNAs, and thus RISC formation (Meister, 2013), we examined the miRNA-loading status of AGO2 in H-RAS^{V12}-expressing cells. We immunopurified AGO2 from control IMR90 cells or from cells expressing PTP1B, H-RAS^{V12}, or both and analyzed AGO2-associated small RNAs by radiolabeling. The association of AGO2 with small RNAs (~22 nt) was readily observed in untransformed cells, but was markedly reduced in H-RAS^{V12}-expressing cells (Figure 3C). Overexpression of PTP1B rescued miRNA loading into AGO2 in H-RAS^{V12}-expressing cells, suggesting that dephosphorylation of AGO2 was required. To test this hypothesis further, we coexpressed AGO2 or AGO2 Tyr 393 mutants with H-RAS^{V12} in *Ago2*-null MEFs and analyzed AGO2-associated small RNAs. Whereas WT and Y393F mutant

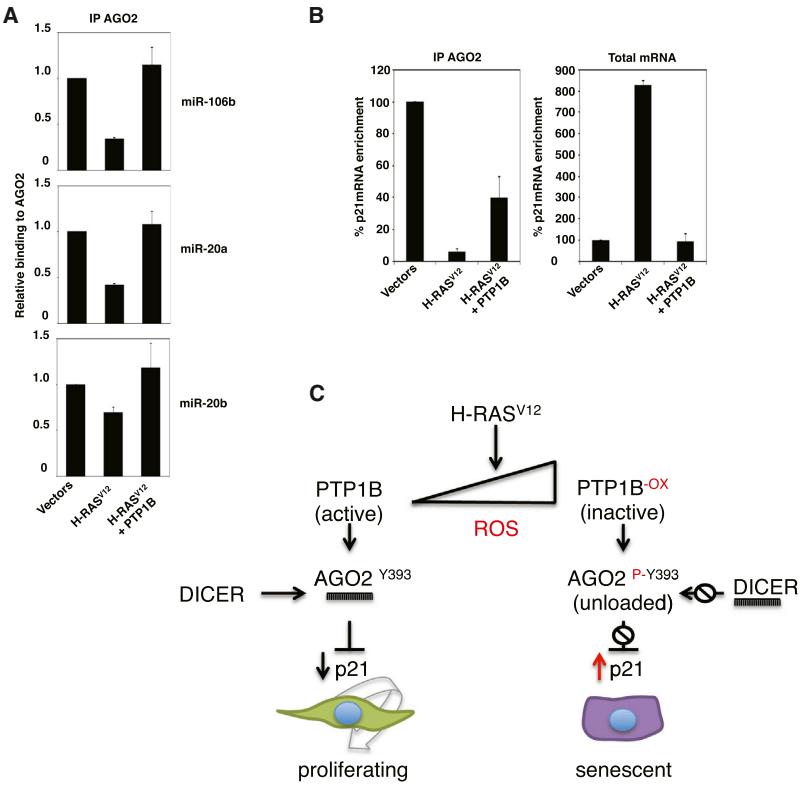

Figure 4. Phosphorylation of AGO2 on Tyr 393 Prevented MicroRNA Loading and Post-transcriptional Repression of p21

(A) AGO2 was immunoprecipitated from lysates of IMR90 cells, infected with control vectors, *H-RAS*^{V12} alone, or coinfected with *PTP1B WT*, and AGO2-associated miRNAs were extracted. After cDNAs were synthesized, miR-20a, -20b, and -106b were assessed by qRT-PCR. Enrichment of miRNA was normalized to 1 in IMR90 fibroblasts.

(B) AGO2 was immunoprecipitated from lysates of IMR90 cells infected with control vectors, *H-RAS*^{V12} alone, or coinfected with *PTP1B* WT. AGO2-associated RNAs were extracted, and cDNA was synthesized and used for qRT-PCR to detect p21. Enrichment levels of p21 mRNA were normalized to 100% in IMR90 fibroblasts.

(C) Schematic model of ROS regulation of PTP1B and AGO2 activity in H-RAS^{V12}-mediated senescence. Error bars represent SEM (n = 3).

AGO2 were associated with endogenous small RNAs, this association was dramatically decreased with the Y393D mutant (Figure 3D). Taken together, our data suggest that increased phosphorylation of AGO2 on Tyr 393 prevented association of AGO2 with miRNAs and thus miRNA-mediated gene silencing.

AGO2 Tyrosine 393 Phosphorylation Prevented Silencing of p21 in *H-RAS*^{V12}-Transformed Fibroblasts

To examine further the effect of H-RAS^{V12} expression on gene silencing, total RNA from IMR90 fibroblasts and IMR90 fibroblasts expressing H-RAS^{V12} were hybridized to microarrays that report the expression status of 1,105 human miRNAs (Figure S4A). Transformation of human diploid fibroblasts with *H-RAS*^{V12} resulted in induction of oncogenic miRNAs. Members of the oncogenic miR-17∼92 cluster and its two paralogs, the miR106a∼363 and miR106b∼25 clusters (18a, 19b, 20a, 20b, 106b), were among the top 20 upregulated miRNAs (Figure S4A). These miRNAs promote cell cycle progression by cooperative downregulation of p21 mRNA (Olive et al., 2010). Our results indicate *H-RAS*^{V12}-induced upregulation of p21 protein (Figures 1F and 2F). To test if this increase in p21 protein resulted from decreased silencing by miRNAs, we characterized miRNAs associated with AGO2 in control or H-RAS^{V12}-expressing IMR90 cells in the presence and absence of coexpressed PTP1B, and quantitated levels of AGO2-associated miR-20a, -20b, and -106b by qPCR. In accordance with our observations on global AGO2 loading with small RNAs (Figures 3C and 3D), the association of AGO2 with these miRNAs was decreased by H-RAS^{V12} signaling. Coexpression of WT PTP1B recovered loading of AGO2 with all three miRNAs (Figures 4A, S4B, and S4C).

To evaluate the effects on AGO2-p21 mRNA interactions, we immunoprecipitated AGO2 and performed qPCR on p21 mRNA from control IMR90 cells, or from IMR90 cells expressing H-RAS^{V12} in the presence and absence of coexpressed PTP1B. AGO2-p21 mRNA interaction was maximal in control IMR90 cells, whereas expression of H-RAS^{V12} decreased this interaction by >90% (Figure 4B). Furthermore, p21 mRNA levels were increased 8-fold in H-RAS^{V12}-expressing cells compared to untransformed fibroblasts (Figure 4B, right panel). Overexpression of PTP1B together with H-RAS^{V12} restored the association of AGO2 with p21 mRNA to ∼40% of the level observed in nonsenescent cells, suggesting re-establishment of an active RISC. Accordingly, levels of p21 mRNA were silenced to a similar extent as in control IMR90 cells. Taken together, our data suggest a model for H-RAS^{V12}-induced senescence that involves derepression of p21 mRNA levels due to inhibition of miRNA silencing as a consequence of PTP1B oxidation by ROS and enhanced tyrosine phosphorylation of AGO2 (Figure 4C).

DISCUSSION

Elevated expression of the *RAS* oncogene initiates a premature senescence program in cultured cells and in vivo that limits the mitogenicity of excessive RAS signaling (Collado and Serrano, 2010; Ferbeyre, 2007; Serrano et al., 1997). Our results demonstrate that RAS-triggered generation of ROS was an integral part of the signaling events leading to oncogene-induced cell-cycle arrest by causing the inactivation of PTP1B, a direct regulator of AGO2 activity. We have shown that expression of members of the miR-17∼92 family, known to play a role in several cancers

(Olive et al., 2010), were elevated in RAS-expressing cells. Importantly, the reversible oxidation and inactivation of PTP1B resulted in enhanced phosphorylation and inactivation of AGO2. In turn, the inactivated AGO2 was uncoupled from DICER, and consequently unloaded of miRNAs, which was a direct cause of elevated expression of p21. Therefore, redox regulation of PTP1B overrode the *RAS* oncogenic program, via inactivation of AGO2, which led to senescence.

Previous reports have linked PTP1B function to regulation of the RAS/ERK pathway downstream of growth factor signaling; it was shown that loss of PTP1B led to decreased RAS activation and signaling upon growth factor receptor activation (Julien et al., 2011). Our data also implicate PTP1B as a regulator of AGO2 downstream of oncogenic RAS signaling in senescence. In our hands, expression of an activated *RAS* allele (*H-RAS*^{V12}), to trigger RAS oncogenic signaling in primary human diploid fibroblasts, bypassed this effect of PTP1B upstream of RAS. Hence, cancer cells affected by gain-of-function mutations in the *RAS* gene may depend on PTP1B-mediated dephosphorylation of Tyr 393 in AGO2 to limit the effects of excessive RAS signaling. Interestingly, increased PTP1B expression has been reported in various cancers (Julien et al., 2011), which may contribute to progression by suppressing AGO2 Tyr 393 phosphorylation and senescence. It is noteworthy that expression of a catalytically inactive PTP1B or an AGO2 pseudo-phospho Tyr 393 mutant was not sufficient in itself to cause senescence; hence, inhibiting PTP1B alone would not be expected to induce senescence.

AGO2 is tightly regulated by posttranslational modifications. Phosphorylation at serine 387 by AKT3 mediates its localization at P-bodies and upregulates translational repression of miRNA targets (Horman et al., 2013; Zeng et al., 2008). Conversely, phosphorylation of AGO2 at Tyr 529, which has been proposed to occur during RISC disassembly, prevents efficient binding of small RNAs (Rüdel et al., 2011). A third phosphorylation site, Tyr 393, has also been identified (Rüdel et al., 2011; Shen et al., 2013). Using a model of hypoxic stress, Shen et al. reported that AGO2 was associated with the epidermal growth factor receptor, which directly phosphorylated AGO2 on Tyr 393 (Shen et al., 2013). In turn, this led to the dissociation of AGO2 and DICER, inhibited the maturation of miRNAs, enhanced cell survival and invasiveness, and correlated with poor survival in breast cancer patients. Interestingly, PTP1B transcription is repressed by HIF in hypoxic stress, consistent with reduced PTP1B activity and the potential for phosphorylation of AGO2 on Tyr 393 in these conditions (Shen et al., 2013; Suwaki et al., 2011). In our study, the interaction of DICER and AGO2 was dependent on PTP1B expression in cells expressing oncogenic RAS, with phosphorylation of Tyr 393 required for decreased association of AGO2 and DICER. AGO2 can bind single-stranded siRNAs in vitro (Rivas et al., 2005); however, endogenous loading of small RNAs requires formation of a functional RISC loading complex that at its core consists of DICER and AGO2 (Meister, 2013). Hence, the dissociation of AGO2 from DICER would be expected to impair miRNA loading into AGO2.

Proteins of the RNAi pathway are found in most subcellular compartments. Although there is no consensus on the exact subcellular sites of RNA silencing, a recent report investigating this aspect of RNAi biology found that mi- and siRNA loaded AGO2, DICER, and TRBP almost exclusively cosedimented with the markers of the rough ER membranes (Stalder et al., 2013), where PTP1B is also localized (Frangioni et al., 1992). The proximity of active PTP1B and an ER-anchored RISC complex may be sufficient to keep AGO2 in an active state. Additionally, it is worth noting that argonaute proteins and mature miRNAs are mutually dependent on each other for their stability (Martinez and Gregory, 2013; Zamudio et al., 2014). However, we observe stable protein levels of unloaded AGO2 in the phosphorylated state, similar to previous observations (Shen et al., 2013). Hence, phosphorylation of AGO2 at Tyr 393 appears to abolish the dependence of AGO2 protein stability on association with mature miRNAs, and on functional RISC formation.

Various miRNAs modulate gene expression programs central to senescence (Gorospe and Abdelmohsen, 2011). Upregulation of miRNAs such as the miR-106b family was shown to overcome H-RAS^{V12}-induced senescence by silencing p21 and other cell cycle regulators in human mammary epithelial cells (Borgdorff et al., 2010). Gene silencing by miRNAs can be shaped by qualitative changes in miRNA profiles, or globally by activation or inhibition of core protein factors (Lujambio and Lowe, 2012). Our data suggest that inhibition of overall miRNA silencing as a consequence of PTP1B inactivation can prevent the action of oncogenic miRNAs and preserve a senescence program.

Overall, the pathway delineated herein reveals PTP1B as a critical checkpoint in oncogenic RAS signaling. Our observations contribute to a better understanding of the induction of senescence in response to oncogenic RAS signaling in primary human fibroblasts and contribute further to the growing body of evidence that the activity of miRNA silencing is highly regulated posttranslationally.

EXPERIMENTAL PROCEDURES

Cell Culture and Reagents

IMR90 cells were cultured in DMEM containing 10% FBS and penicillin/streptomycin and 10% nonessential amino acids. MEFs and HEK293 cells were cultured in DMEM containing 10% FBS and penicillin/streptomycin. Antibodies and other reagents are described in Supplemental Information. The experimental protocol conformed to the Guide for the Care and Use of Laboratory Animals published by the NIH (NIH Publication No. 85-23, revised 1996).

Assay of PTP Oxidation

The cysteinyl-labeling assay of reversibly oxidized PTPs was performed as previously described in Boivin et al. (2010).

β-Galactosidase Activity Staining

SA β-gal activity was measured as previously described (Serrano et al., 1997) and presented as the percentage of senescent cells in each sample relative to the total number of cells.

Immunoblotting

Lysates or immunoprecipitates were separated by SDS-PAGE, transferred onto nitrocellulose membranes, and probed with the indicated antibodies. A CAPS transfer buffer was used to transfer AGO2, whereas a Tris-glycine transfer buffer was used for all other proteins. Membranes were blotted as previously described (Boivin et al., 2008).

PTP Substrate-Trapping Assay

Cells coexpressing the PTP1B-trapping mutant or wild-type PTP1B were lysed, and PTP1B was immunoprecipitated and washed with trapping lysis

buffer and PBS (Tonks, 2013). Analysis of the immune complexes was performed by LC-MS/MS and by immunoblotting.

Measurement of miRNA Association with AGO2

AGO2 was immunoprecipitated, and RNAs were extracted from the immunoprecipitates using Trizol. Following extraction, the 5′ phosphates of the RNAs were removed, and the 5′-end was phosphorylated using [γ-^{32}P]-ATP. The 5′-labeled RNAs were resolved by urea-PAGE, gels were dried, and the radiograph was analyzed using a Fuji phosphorimager.

Quantitation of AGO2-Bound miRNAs and mRNAs

AGO2-bound RNAs were quantitated by qRT-PCR. Briefly, RNAs from immunoprecipitated AGO2 and lysates were extracted using Trizol, treated with DNase, and cDNAs were generated. The cDNA library was then used as a template for qRT-PCR using a SYBR Green master mix. GAPDH was used as an internal control. For quantitation, each miRNA and U6 snRNA was reverse transcribed, and cDNAs were used for qPCR. U6 snRNA was used as internal control.

Details of materials and methods are described in Supplemental Experimental Procedures.

SUPPLEMENTAL INFORMATION

Supplemental Information includes four figures, two tables, and Supplemental Experimental Procedures and can be found with this article online at http://dx.doi.org/10.1016/j.molcel.2014.07.018.

AUTHOR CONTRIBUTIONS

M.Y., B.B., F.-K.H., G.C., and K.D.R. performed experiments. B.C.D. and C.J.C. provided critical reagents. M.Y., B.B., A.D.H., F.-K.H., D.J.P., T.A.N., and N.K.T. designed experiments and analyzed data. B.B., A.D.H., M.Y., and N.K.T. wrote the paper.

ACKNOWLEDGMENTS

We thank Cexiong Fu, Yang Yu, Shipra Das, and the members of the N.K.T. laboratory for helpful discussions. This research was supported by NIH grants CA53840 and GM55989 (N.K.T.), CSHL Cancer Centre Support Grant CA45508 (N.K.T.), NIH grants S10RR027990 and P30CA016087 (T.A.N.), and NIH grant GM 79465 (C.J.C). N.K.T. is also grateful for support from the following foundations: The Gladowsky Breast Cancer Foundation, The Don Monti Memorial Research Foundation, Hansen Memorial Foundation, West Islip Breast Cancer Coalition for Long Island, Glen Cove CARES, Find a Cure Today (FACT), Constance Silveri, Robertson Research Fund, and the Masthead Cove Yacht Club Carol Marcincuk Fund. B.B. was supported by the Fonds de Recherche de l'Institut de Cardiologie de Montréal and the Heart and Stroke Foundation-Quebec. A company called DepYmed, Inc. was founded on March 3, 2014. It is owned 50-50 by Ohr Pharmaceuticals and Cold Spring Harbor Lab. The goal of the company is to take an inhibitor of PTP1B, MSI-1436/trodusquemine, into clinical trials in HER2-positive breast cancer patients. Based upon the conditions of the invention agreement signed by all scientists at Cold Spring Harbor Lab, the senior author, N.K.T., would be entitled to a share. Nevertheless, at this time no funds have been raised to support the efforts of the company.

Received: January 21, 2014
Revised: May 29, 2014
Accepted: July 21, 2014
Published: August 28, 2014

REFERENCES

Boivin, B., Zhang, S., Arbiser, J.L., Zhang, Z.Y., and Tonks, N.K. (2008). A modified cysteinyl-labeling assay reveals reversible oxidation of protein tyrosine phosphatases in angiomyolipoma cells. Proc. Natl. Acad. Sci. USA *105*, 9959–9964.

Boivin, B., Yang, M., and Tonks, N.K. (2010). Targeting the reversibly oxidized protein tyrosine phosphatase superfamily. Sci. Signal. *3*, pl2.

Borgdorff, V., Lleonart, M.E., Bishop, C.L., Fessart, D., Bergin, A.H., Overhoff, M.G., and Beach, D.H. (2010). Multiple microRNAs rescue from Ras-induced senescence by inhibiting p21(Waf1/Cip1). Oncogene *29*, 2262–2271.

Brown, D.I., and Griendling, K.K. (2009). Nox proteins in signal transduction. Free Radic. Biol. Med. *47*, 1239–1253.

Collado, M., and Serrano, M. (2010). Senescence in tumours: evidence from mice and humans. Nat. Rev. Cancer *10*, 51–57.

DeNicola, G.M., and Tuveson, D.A. (2009). RAS in cellular transformation and senescence. Eur. J. Cancer *45* (*Suppl 1*), 211–216.

Dickinson, B.C., Peltier, J., Stone, D., Schaffer, D.V., and Chang, C.J. (2011). Nox2 redox signaling maintains essential cell populations in the brain. Nat. Chem. Biol. *7*, 106–112.

Ferbeyre, G. (2007). Barriers to Ras transformation. Nat. Cell Biol. *9*, 483–485.

Finkel, T. (2011). Signal transduction by reactive oxygen species. J. Cell Biol. *194*, 7–15.

Frangioni, J.V., Beahm, P.H., Shifrin, V., Jost, C.A., and Neel, B.G. (1992). The nontransmembrane tyrosine phosphatase PTP-1B localizes to the endoplasmic reticulum via its 35 amino acid C-terminal sequence. Cell *68*, 545–560.

Gorospe, M., and Abdelmohsen, K. (2011). Microregulators come of age in senescence. Trends Genet. *27*, 233–241.

Hanahan, D., and Weinberg, R.A. (2000). The hallmarks of cancer. Cell *100*, 57–70.

Horman, S.R., Janas, M.M., Litterst, C., Wang, B., MacRae, I.J., Sever, M.J., Morrissey, D.V., Graves, P., Luo, B., Umesalma, S., et al. (2013). Akt-mediated phosphorylation of argonaute 2 downregulates cleavage and upregulates translational repression of microRNA targets. Mol. Cell *50*, 356–367.

Irani, K., Xia, Y., Zweier, J.L., Sollott, S.J., Der, C.J., Fearon, E.R., Sundaresan, M., Finkel, T., and Goldschmidt-Clermont, P.J. (1997). Mitogenic signaling mediated by oxidants in Ras-transformed fibroblasts. Science *275*, 1649–1652.

Julien, S.G., Dubé, N., Hardy, S., and Tremblay, M.L. (2011). Inside the human cancer tyrosine phosphatome. Nat. Rev. Cancer *11*, 35–49.

Krishnan, N., Koveal, D., Miller, D.H., Xue, B., Akshinthala, S.D., Kragelj, J., Jensen, M.R., Gauss, C.M., Page, R., Blackledge, M., et al. (2014). Targeting the disordered C terminus of PTP1B with an allosteric inhibitor. Nat. Chem. Biol. *10*, 558–566.

Lee, A.C., Fenster, B.E., Ito, H., Takeda, K., Bae, N.S., Hirai, T., Yu, Z.X., Ferrans, V.J., Howard, B.H., and Finkel, T. (1999). Ras proteins induce senescence by altering the intracellular levels of reactive oxygen species. J. Biol. Chem. *274*, 7936–7940.

Lujambio, A., and Lowe, S.W. (2012). The microcosmos of cancer. Nature *482*, 347–355.

Mark, T.B., Blaskovich, A.T., Baughman, T., Little, T., Patt, W., Qaber, M., Schultz, L.M., Nagula, G., Gage, J.L., and Howbert, J.J. June 2006. Protein tyrosine phosphatase inhibitors and methods of use thereof. U.S. patent US2006142250(A1).

Martinez, N.J., and Gregory, R.I. (2013). Argonaute2 expression is post-transcriptionally coupled to microRNA abundance. RNA *19*, 605–612.

Meister, G. (2013). Argonaute proteins: functional insights and emerging roles. Nat. Rev. Genet. *14*, 447–459.

Olive, V., Jiang, I., and He, L. (2010). mir-17-92, a cluster of miRNAs in the midst of the cancer network. Int. J. Biochem. Cell Biol. *42*, 1348–1354.

Rhee, S.G. (2006). Cell signaling. H2O2, a necessary evil for cell signaling. Science *312*, 1882–1883.

Rivas, F.V., Tolia, N.H., Song, J.J., Aragon, J.P., Liu, J., Hannon, G.J., and Joshua-Tor, L. (2005). Purified Argonaute2 and an siRNA form recombinant human RISC. Nat. Struct. Mol. Biol. *12*, 340–349.

Rüdel, S., Wang, Y., Lenobel, R., Körner, R., Hsiao, H.H., Urlaub, H., Patel, D., and Meister, G. (2011). Phosphorylation of human Argonaute proteins affects small RNA binding. Nucleic Acids Res. *39*, 2330–2343.

Schubbert, S., Shannon, K., and Bollag, G. (2007). Hyperactive Ras in developmental disorders and cancer. Nat. Rev. Cancer *7*, 295–308.

Serrano, M., Lin, A.W., McCurrach, M.E., Beach, D., and Lowe, S.W. (1997). Oncogenic ras provokes premature cell senescence associated with accumulation of p53 and p16INK4a. Cell *88*, 593–602.

Shen, J., Xia, W., Khotskaya, Y.B., Huo, L., Nakanishi, K., Lim, S.O., Du, Y., Wang, Y., Chang, W.C., Chen, C.H., et al. (2013). EGFR modulates microRNA maturation in response to hypoxia through phosphorylation of AGO2. Nature *497*, 383–387.

Stalder, L., Heusermann, W., Sokol, L., Trojer, D., Wirz, J., Hean, J., Fritzsche, A., Aeschimann, F., Pfanzagl, V., Basselet, P., et al. (2013). The rough endoplasmatic reticulum is a central nucleation site of siRNA-mediated RNA silencing. EMBO J. *32*, 1115–1127.

Suwaki, N., Vanhecke, E., Atkins, K.M., Graf, M., Swabey, K., Huang, P., Schraml, P., Moch, H., Cassidy, A.M., Brewer, D., et al. (2011). A HIF-regulated VHL-PTP1B-Src signaling axis identifies a therapeutic target in renal cell carcinoma. Sci. Transl. Med. *3*, 85ra47.

Tonks, N.K. (2013). Protein tyrosine phosphatases—from housekeeping enzymes to master regulators of signal transduction. FEBS J. *280*, 346–378.

Zamudio, J.R., Kelly, T.J., and Sharp, P.A. (2014). Argonaute-bound small RNAs from promoter-proximal RNA polymerase II. Cell *156*, 920–934.

Zeng, Y., Sankala, H., Zhang, X., and Graves, P.R. (2008). Phosphorylation of Argonaute 2 at serine-387 facilitates its localization to processing bodies. Biochem. J. *413*, 429–436.